

# Improved field emission properties of carbon nanotube cathodes by nickel electroplating and corrosion\*

Xiao Xiaojing(肖晓晶), Ye Yun(叶芸)<sup>†</sup>, Zheng Longwu(郑隆武), and Guo Tailiang(郭太良)<sup>†</sup>

Institute of Optoelectronic Display Technology, School of Physics and Information Engineering, Fuzhou University, Fuzhou 350002, China

**Abstract:** Carbon nanotube (CNT) cathodes prepared by electrophoretic deposition were treated by a combination of nickel electroplating and cathode corrosion technologies. The characteristics of the samples were measured by scanning electron microscopy, energy dispersive X-ray spectroscopy,  $J-E$  and  $F-N$  plots. After the treatment, the CNT cathodes showed improved field emission properties such as turn-on field, threshold electric field, current density, stability and luminescence uniformity. Concretely, the turn-on field decreased from 0.95 to 0.45 V/ $\mu\text{m}$  at an emission current density of 1 mA/cm<sup>2</sup>, and the threshold electric field decreased from 0.99 to 0.46 V/ $\mu\text{m}$  at a current density of 3 mA/cm<sup>2</sup>. The maximum current density was up to 7 mA/cm<sup>2</sup> at a field of 0.48 V/ $\mu\text{m}$ . In addition, the current density of the CNT cathodes fluctuated at around 0.7 mA/cm<sup>2</sup> for 20 h, with an initial current density 0.75 mA/cm<sup>2</sup>. The improvement in field emission properties was found to be due to the exposure of more CNT tips, the wider gaps among the CNTs and the infiltration of nickel particles.

**Key words:** carbon nanotube; cathode corrosion; Ni electroplating; field emission

**DOI:** 10.1088/1674-4926/33/5/053004

**PACC:** 7970; 8160; 6148

## 1. Introduction

Since the first report in 1991<sup>[1]</sup>, carbon nanotubes (CNTs) have attracted enormous interest around the world in many fields due to their outstanding optical, electrical and mechanical properties. Owing to their special geometrical properties, including high aspect ratio and small tip radii of curvature, CNTs have also been thought of as ideal field emission materials. Presently, chemical vapor deposition (CVD)<sup>[2,3]</sup>, screen-printing<sup>[4,5]</sup> and electrophoretic deposition (EPD)<sup>[6]</sup> are generally used for the preparation of CNT cathodes. However, the CVD method requires high vacuum and growth temperature, which limits the substrate selectivity. The screen-printing method introduces an organic additive into the CNT film, which leads to a negative effect on the field emission performance of the CNT cathode. Besides, the uniformity and thickness of CNT films are not easily controlled. In contrast, the EPD method is simple but robust because of its low process temperature and the possibility of scale-up<sup>[7]</sup>. Moreover, it offers better uniformity of the CNT film than that of screen-printing. But the good field emission properties of CNT films by EPD cannot be guaranteed because of the CNT tips lying on the surface of the film<sup>[8,9]</sup>, the compactness among the CNT<sup>[10,11]</sup> and the high barrier between the CNT and substrate<sup>[12]</sup>.

Due to these shortfalls in CNT films by EPD, both domestic and foreign scholars have researched the method of composite electrodeposition to improve the field emission properties of CNT films<sup>[13-15]</sup>. Fan *et al.*<sup>[16]</sup> used the CNT/nickel (Ni) composite electrophoretic deposition method to improve the field

emission properties of CNT cathodes. This method is effective and simple but there are still many disadvantages. For example, the CNTs in the composites would be easily covered by the consequently deposited nanoparticles in the process, which leads to a decrease in the effective field emitters in the CNT cathode. Moreover, this method cannot guarantee wide gaps between the CNTs.

In this study, an effective treatment of a combination of Ni electroplating and cathode corrosion is demonstrated. On the one hand, Ni electroplating decreases the barrier between the CNT and the substrate electrode<sup>[17]</sup>, and on the other, cathode corrosion widens the gaps between the CNTs and exposes more CNT tips to air. Therefore, the field emission characteristics of the CNT film are improved after the treatment.

## 2. Experiments

### 2.1. Cathode preparation

Multi-walled CNTs with a diameter of 10–20 nm, a length of 5–15 nm and a purity  $\geq 95\%$  were purchased from Shenzhen Nanoport Company. Purification is necessary before the next step of the experiment since the raw CNTs were often aggregated and/or entangled with many impurities such as amorphous carbon and catalytic metal particles. The CNT purification process was as follows: initially, raw CNTs were stirred in a concentrated HNO<sub>3</sub> and H<sub>2</sub>SO<sub>4</sub> solution (1 : 3 volume ratios) at 100 °C for 4 h. Then, acid-treated CNTs were washed with demonized water to become neutral and dried at 120 °C for 30 min to form the purified CNTs.

\* Project supported by the National High Technology Research and Development Program of China (No. 2008AA03A313), the National Natural Science Foundation of China (No. 61106053), and the Specialized Research Fund for the Doctoral Program of Higher Education of China (No. 20103514110007).

<sup>†</sup> Corresponding author. Email: yeyun07@fzu.edu.cn, gtl\_fzu@yahoo.com.cn

Received 30 September 2011, revised manuscript received 28 November 2011

© 2012 Chinese Institute of Electronics

Afterwards, the purified CNTs were used for the EPD process. The CNT electrophoretic suspension (composed of 20 mg purified CNT powders, 200 mL propyl alcohol and 50 mg  $\text{Mg}(\text{NO}_3)_2 \cdot 6\text{H}_2\text{O}$ ) was produced after ultrasonic treatment for 60 min at 30 W. The graphite plate was employed as the anode and the CrCuCr film (produced by magnetron sputtering) acted as the cathode. The gap between the two electrodes was around 3 mm. The CNTs were deposited electrophoretically on the surface of the cathode under a current density of  $1 \text{ mA/cm}^2$  for 10 min.

The CNT cathode was followed by Ni electroplating and cathode corrosion treatments. Firstly, for the nickel electroplating process, Ni was electroplated on the CNT film in the plating solution, which was composed of  $\text{NiSO}_4 \cdot 6\text{H}_2\text{O}$  of 10 g/L,  $\text{NiCl}_2 \cdot 6\text{H}_2\text{O}$  of 3 g/L, SDB of 0.001 g/L and  $\text{H}_3\text{BO}_3$  of 40 g/L. The Ni plate was used as the anode and the CNT film prepared by EPD was used as the cathode, respectively. The pH values were adjusted to 5.0 by dilute sulphuric acid and sodium hydroxide. The current density was  $1 \text{ mA/cm}^2$  for 2 min with an electrode gap of 4 cm in the electroplating process. Secondly, for the cathode corrosion method, the CNT/Ni film (prepared by EPD and Ni electroplating) was employed as the anode, and was placed 4 cm away from the cathode (Ni plate). The corrosion process was conducted at a current density of  $0.9 \text{ mA/cm}^2$  for 30 s in the plating solution. After that, all the samples were sintered from room temperature to  $450^\circ\text{C}$  in 99.99%  $\text{N}_2$ , and the temperature was kept at  $450^\circ\text{C}$  in 99.99%  $\text{N}_2$  for 30 min to remove organic additives. Finally, the samples were cooled down from  $450^\circ\text{C}$  to room temperature in  $\text{N}_2$  gas.

## 2.2. Characterization methods

The morphologies and chemical composition of the samples were examined by scanning electron microscopy (SEM, HITACHI S-3000) equipped with an energy dispersive X-ray spectroscope (EDX, EDAX GENESIS). The field emission properties and the stability of the samples were measured in a diode structure under a  $3.7 \times 10^{-9}$  Torr vacuum with a spacer height of  $1100 \mu\text{m}$ . The dimensions of the fabricated samples were  $5 \times 4 \text{ cm}^2$ . The indium tin oxide glasses printed with green phosphor were used as the anode.

## 3. Results and discussion

Schematic diagrams of CNT electrophoretic deposition, Ni electroplating and cathode corrosion are shown in Fig. 1. In Fig. 1(a), the charged CNTs in the suspension move and are deposited on the CrCuCr electrode to form the CNT film, under a constant current density. In Fig. 1(b), under a constant current density at  $1 \text{ mA/cm}^2$  for 2 min,  $\text{Ni}^{2+}$  ions gradually travel through the Ni plating solution and infiltrate into the CNT film to form the CNT/Ni film<sup>[18]</sup>. In Fig. 1(c), the anode is the CNT/Ni film and the cathode is the Ni plate. With a constant current density of  $0.9 \text{ mA/cm}^2$  between the cathode and the anode, an electric field is produced by the voltage and a magnetic field is produced by the electric current. Because of the current and acid plating the Ni solution, the Ni nanoparticles in the plating solution are dissolved from the surface of the CNT/Ni film and become  $\text{Ni}^{2+}$  ions to form the dissolved CNT/Ni film. Then, due to the effect of the electric field,  $\text{Ni}^{2+}$

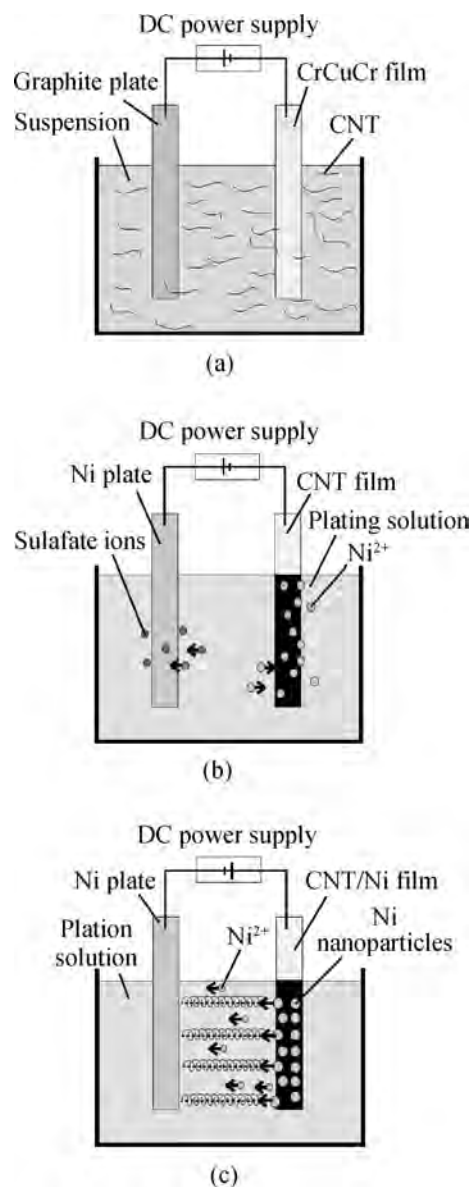


Fig. 1. Schematic diagram of (a) CNT electrophoretic deposition, (b) Ni electroplating, and (c) cathode corrosion.

ions move to the cathode through the plating solution. Because of the magnetic field, Ni nanoparticles are magnetized and directed to the cathode. At the same time, some CNTs (encased with Ni nanoparticles) in the CNT/Ni film are directed to the cathode from the surface. Because of this, more CNT tips are exposed and the relative CNT content of the dissolved CNT/Ni film is increased compared with that of the CNT/Ni film.

### 3.1. Morphological properties

Figure 2 illustrates the surface morphology of the fabricated films, showing: (a) a top view of the EPD CNT film, (b) a top view of the CNT/Ni film, (c) a top view of the dissolved CNT/Ni film, (d) a side view of the EPD CNT film, and (e) a side view of the dissolved CNT/Ni film. In Fig. 2(a), CNTs were deposited in a substrate electrode by electrophoretic deposition. Figure 2(b) shows that after Ni electroplating the surfaces of the nanotubes were coated with Ni nanoparticles. Figure 2(c) is an SEM image of the CNT/Ni film after cath-

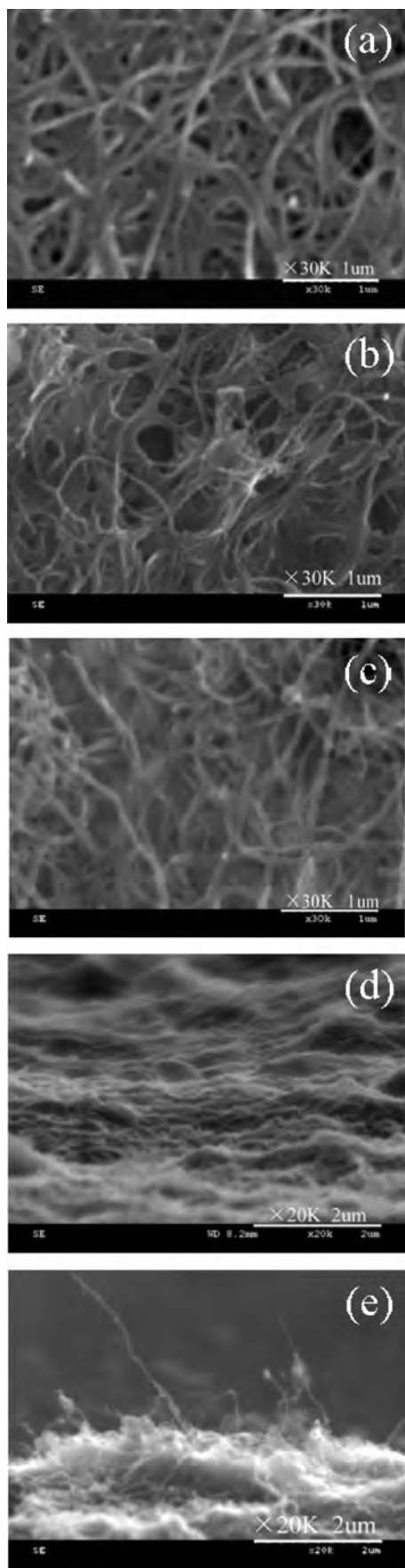


Fig. 2. SEM images of (a) a top view of the EPD CNT film, (b) a top view of the CNT/Ni film, (c) a top view of the dissolved CNT/Ni film, (d) a side view of the EPD CNT film, and (e) a side view of the dissolved CNT/Ni film.

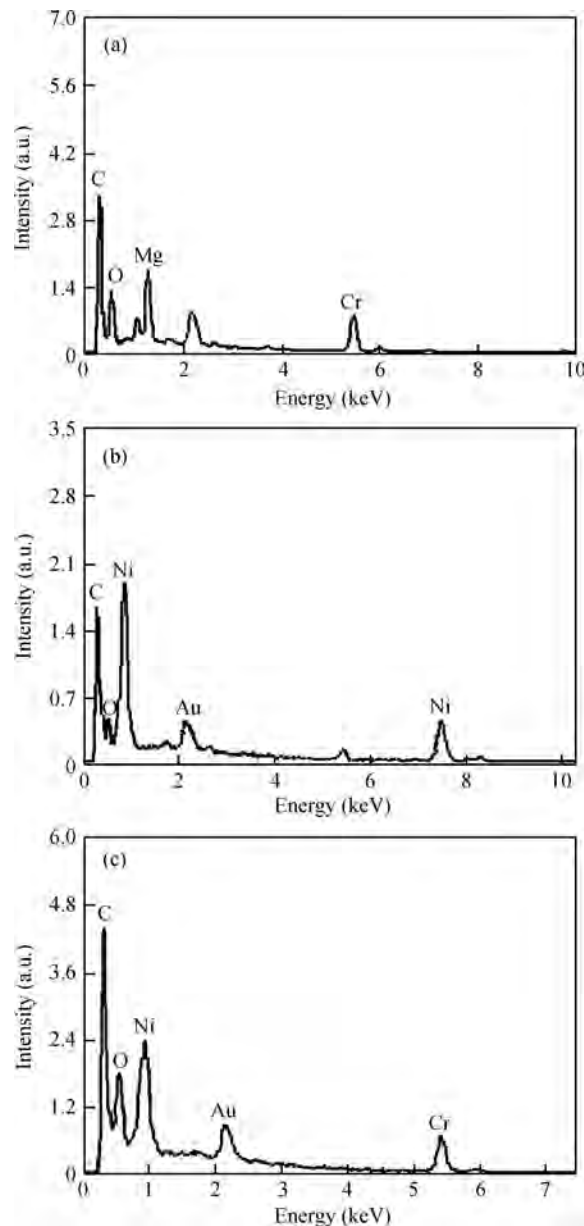


Fig. 3. EDX analyses of (a) the EPD CNT film, (b) the CNT/Ni film, and (c) the dissolved CNT/Ni film.

ode corrosion. In contrast to Fig. 2(b), Figure 2(c) shows that the Ni nanoparticles on the surface of the CNT were dissolved through the cathode corrosion method. It was also found from Fig. 2(c) that the cathode corrosion method widened the gaps among the CNTs (compared to Fig. 2(a)), which resulted in a decrease in the electric field shield effect among the CNTs<sup>[10, 11]</sup>. Figure 2(d) is a side view of the EPD CNT film. No sharp CNT tips can be clearly seen in the SEM side view of the EPD CNT film, whereas there were some tips on the surface of the CNT film after cathode corrosion, and more tips were exposed to the surface of the composite film, as can be seen from Fig. 2(e).

The chemical composition of the samples was analyzed by EDX. Figure 3(a) shows carbon, oxygen, magnesium and chromium. It was obvious that the carbon peak was from the CNTs and the magnesium peak was from the  $Mg(NO_3)_2 \cdot 6H_2O$  in the CNT electrophoretic suspension. In

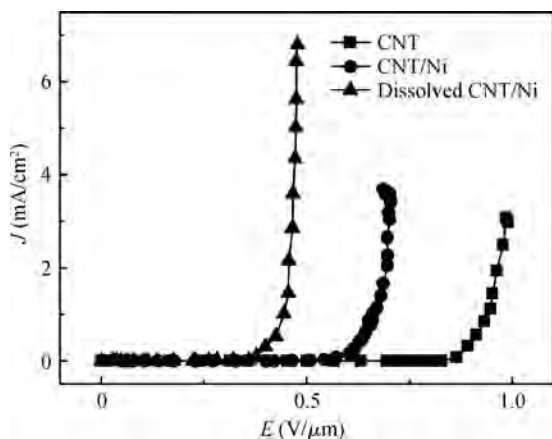


Fig. 4.  $J$ - $E$  plot of field emission current density versus applied electrical field.

addition, the chromium peak was from the substrate. Compared to Fig. 3(a), there were additional Ni and Aurum peaks in the spectrum of Fig. 3(b). The Ni peak was from Ni electroplating and the Aurum peak was from gold sputtering. Compared to Fig. 3(b), the Ni content was decreased and the carbon content was increased in Fig. 3(c) because of the cathode corrosion.

### 3.2. Field emission characteristics

The field emission properties of the CNT, CNT/Ni and dissolved CNT/Ni samples were measured in a vacuum chamber with a pressure of  $3.7 \times 10^{-9}$  Torr, and the anode-cathode distance was about  $1100 \mu\text{m}$ . As can be seen in Fig. 4, the turn-on electric field ( $E_{\text{on}}$ , defined at an emission current density of  $1 \text{ mA/cm}^2$ ) decreased from  $0.95 \text{ V}/\mu\text{m}$  of the CNT to  $0.66 \text{ V}/\mu\text{m}$  of the CNT/Ni to  $0.45 \text{ V}/\mu\text{m}$  of the dissolved CNT/Ni. Besides, the threshold electric field ( $E_{\text{th}}$ , defined at a current density of  $3 \text{ mA/cm}^2$ ) of the dissolved CNT/Ni film, CNT/Ni film and CNT film were  $0.46$ ,  $0.70$  and  $0.99 \text{ V}/\mu\text{m}$ , respectively. Thus, the dissolved CNT/Ni film had the best field emission properties for the lowest  $E_{\text{on}}$  and the lowest  $E_{\text{th}}$ .

Fowler-Nordheim (F-N) theory<sup>[19]</sup> has proven useful in describing field emission from carbon-based electron emitters. According to the F-N equation, the emission current density is the function of  $E$ ,  $\beta$  and  $\phi$ :

$$J = 1.56 \times 10^{-6} \times \frac{\beta^2 E^2}{\phi} \exp \frac{-6.83 \times 10^7 \phi^{3/2}}{\beta E}, \quad (1)$$

where  $J$  is the field emission current density of the cathodes,  $E$  is the electric field applied between the cathode and the anode,  $\beta$  is the field enhancement factor, and  $\phi$  is the work function of the cathode material. The F-N curve, i.e.  $\ln(J/E^2)$  versus  $1/E$ , is presented in Fig. 5. As the work function  $\phi$  of CNT was  $5.0 \text{ eV}$ <sup>[20]</sup> and the work function  $\phi$  of Ni was  $4.8 \text{ eV}$ , the work function of the CNT/Ni composite was approximately between  $5.0$  and  $4.8 \text{ eV}$ , and was assumed to be  $4.9 \text{ eV}$  in this paper. The field enhancement factors ( $\beta$ ) were determined from the slopes of the  $\ln(J/E^2)$  versus  $1/E$  curve, which were obtained from the linear fittings of Fig. 5. The calculated  $\beta$  values of the dissolved CNT/Ni, the CNT/Ni and the EPD CNT films were  $1.010 \times 10^4$ ,  $8.425 \times 10^3$  and  $4.023 \times 10^3$ , respectively.

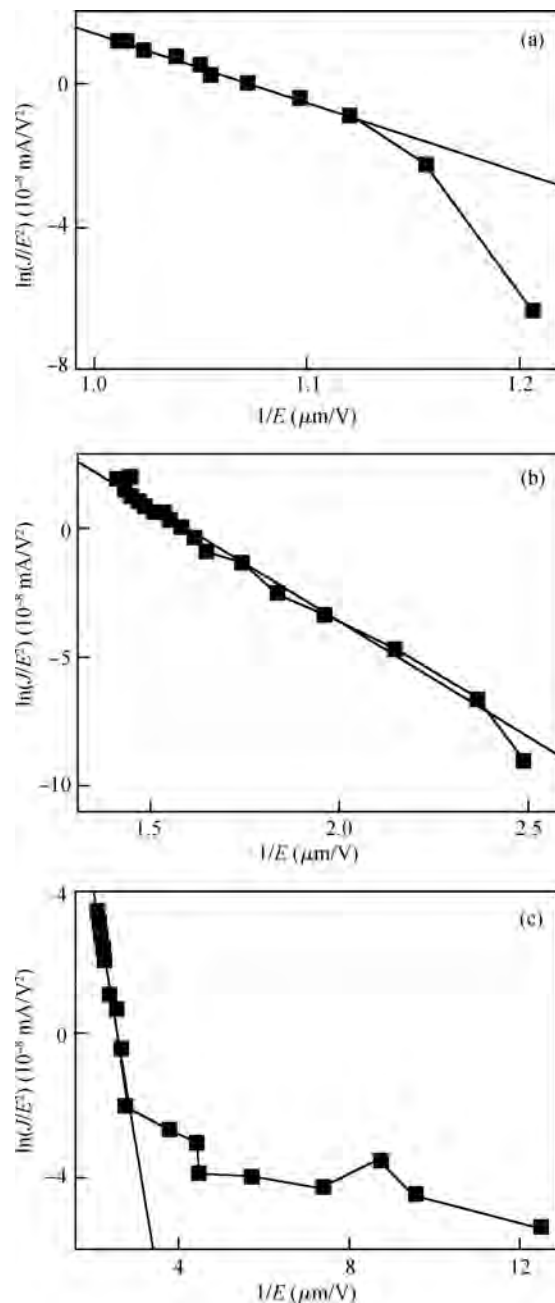


Fig. 5.  $J$ - $E$  properties in the F-N curves of different CNT films at (a) the EPD CNT film, (b) the CNT/Ni film, and (c) the dissolved CNT/Ni film.

Figures 6(a)–6(c) show the field emission images of (a) the EPD CNT film, (b) the CNT/Ni film, and (c) the dissolved CNT/Ni film at DC  $850 \text{ V}$ . In Fig. 6(a), there were few emission sites and the luminescence uniformity was poor. Compared with Fig. 6(a), Figure 6(b) shows more emission sites and better luminescence uniformity. Nevertheless, Figure 6(c) shows the best field emission performance.

There are three reasons for the improvement in CNT film field emission properties after treatment with a combination of Ni electroplating and cathode corrosion. Firstly, the movement of Ni nanoparticles in the plating solution led to more CNT (encased with Ni nanoparticles) exposure to air, which was in favor of electron emitting<sup>[8,21]</sup>. Secondly, the corro-

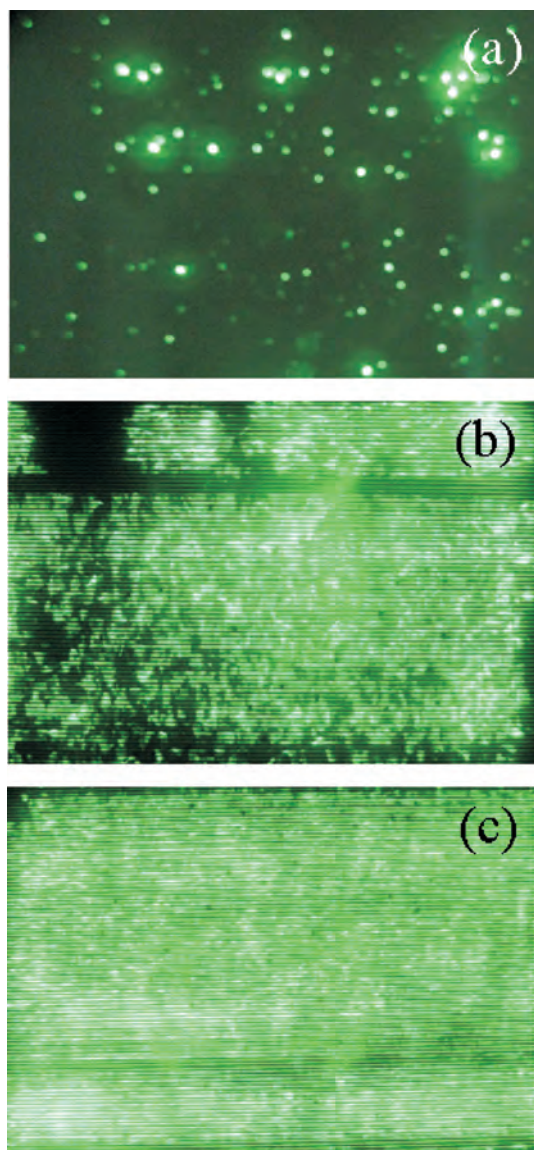


Fig. 6. Field emission images of (a) the EPD CNT film, (b) the CNT/Ni film, and (c) the dissolved CNT/Ni film.

sion of the infiltrated Ni nanoparticles widened the gaps among the CNTs, which led to a decrease in the electric field shield among the CNTs<sup>[10, 11]</sup> and more effective emission sites of the CNT on the cathode. Therefore, the field emission properties of the CNT film were improved. Thirdly, the Ni nanoparticles between the CNTs and the substrate could reduce the contact resistance and lower barrier I. According to the double-barrier potential model<sup>[19]</sup>, the field emission electrons would tunnel through two barriers: barrier I (electrons tunnel through the potential barrier between the substrate and CNT) and barrier II (electrons tunnel through the barrier between the CNT and vacuum). Nickel has good electrical conductivity, so barrier I between the substrate and CNT would decrease, which enhances the field emission properties of the CNTs.

The stability test of the two samples (CNT and dissolved CNT/Ni) is given in Fig. 7. For the two samples, the initial current was set at about 0.75 mA/cm<sup>2</sup> and the testing time was approximately 20 h. As presented in Fig. 7, it was clear that the stability of the dissolved CNT/Ni film was better than that of

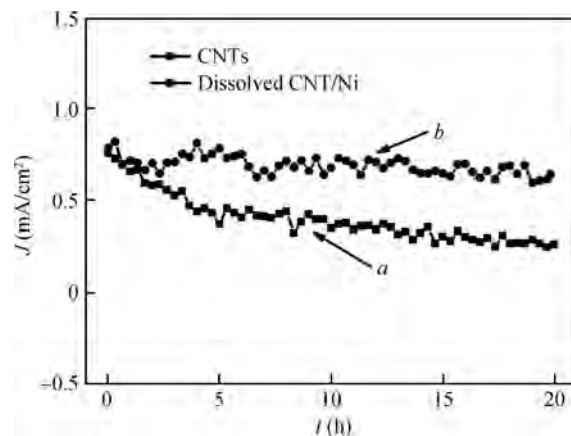


Fig. 7. Emission stability of the CNT film (a) before treatment and (b) after treatment.

the CNT film. After 20 h, the current density of the dissolved CNT/Ni decreased to 82% of the initial current, and the current density of the CNT cathode fluctuated at around 0.7 mA/cm<sup>2</sup>, while that of the CNTs dramatically decreased to 35% of the initial current. Therefore, it was concluded that the treatment of the combination of Ni electroplating and cathode corrosion benefited the field emission properties and the emission stability of the CNT film.

#### 4. Conclusions

CNT films prepared by EPD have the disadvantages of poor field emission properties because of the tips of the CNTs lying on the surface of the film, compactness among the CNTs, and the high barrier between the CNTs and substrate. In order to improve the field emission characteristics of CNT cathodes, treatment with a combination of Ni electroplating and cathode corrosion was employed in this paper. By applying the treatment, most of the CNT tips were exposed to air, the gaps between the CNTs were widened, and the barrier between the CNTs and the substrate was lowered. As a result, the field emission properties, including turn-on field, current density, threshold electric field, emission sites and luminescence uniformity, were improved. CNT cathodes treated by Ni electroplating and cathode corrosion have potential applications in CNT field emission displays and ray tubes.

#### References

- [1] Iijima S. Helical microtubules of graphitic carbon. *Nature*, 1991, 354(6348): 56
- [2] Jayatissa A H, Guo K. Synthesis of carbon nanotubes at low temperature by filament assisted atmospheric CVD and their field emission characteristics. *Vacuum*, 2009, 83(5): 853
- [3] Zhang X Y, Yao N, Wang Y J, et al. Field Emission from a mixture of amorphous carbon and carbon nanotubes films. *Journal of Semiconductors*, 2008, 29(8): 1484
- [4] Qian M, Feng T, Wang K, et al. A comparative study of field emission properties of carbon nanotube films prepared by vacuum filtration and screen-printing. *Appl Surf Sci*, 2010, 256(14): 4642
- [5] Ding H, Feng T, Zhang Z J, et al. Enhanced field emission properties of screen-printed doubled-walled carbon nanotubes by poly-

- dimethylsiloxane elastomer. *Appl Surf Sci*, 2010, 256(22): 6596
- [6] Wang L L, Chen Y W, Chen T, et al. Optimization of field emission properties of carbon nanotubes cathodes by electrophoretic deposition. *Mater Lett*, 2007, 61(4/5): 1265
- [7] Fowler R H. The analysis of photoelectric sensitivity curves for clean metals at various temperatures. *Phys Rev*, 1931, 38(1): 45
- [8] Zhang W F, Zeng B Q, Zhao Y H, et al. Study on field emission properties of CNTs/PTFE composite materials. *Func Mater*, 2006, 37(7): 1118 (in Chinese)
- [9] Dong J H, Shan Y. Field emission properties of carbon nanotubes/diamond composite. *Chinese Journal of Luminescence*, 2010, 31(4): 597 (in Chinese)
- [10] Li X, He Y N, Liu W H, et al. Improving carbon nanotube field emission display luminescence uniformity by introducing a reactive current limiting layer. *Journal of Semiconductors*, 2008, 29(3): 575 (in Chinese)
- [11] Liao Q L, Zhang Y, Xia L S, et al. Research on intense pulsed emission of carbon nanotube cathode. *Acta Physica Sinica*, 2007, 56(9): 5335 (in Chinese)
- [12] Chen L F, Ji Z G, Mi Y H, et al. Effect of interface barrier on carbon nanotube field emission properties. *High Power Laser and Particle Beams*, 2009, 22(2): 397 (in Chinese)
- [13] Zheng L W, Hu L Q, Yang F, et al. Improvement of the field emission properties of carbon nanotubes by CNT/Fe<sub>3</sub>O<sub>4</sub> composite electrophoretic deposition. *Journal of Semiconductors*, 2011, 32(12): 126001
- [14] Deng M, Ding G F, Wang Y, et al. Room temperature mass production of carbon nanotube field emission micro-cathode arrays using electroplating of CNT/Ni composite followed by micromachining. *Vacuum*, 2010, 85(8): 827
- [15] Deng Min, Ding Guifu, Wang Yan, et al. Fabrication of Ni-matrix carbon nanotube field emitters using composite electroplating and micromachining. *Carbon*, 2009, 47(15): 3466
- [16] Fan Y C, Liu Y M, Chen Y C, et al. Carbon nanotube field emission cathodes fabricated with chemical displacement plating. *Appl Surf Sci*, 2009, 255(17): 7753
- [17] Ngo Q, Petranovic D, Krishnan S, et al. Electron transport through metal-multiwall carbon nanotube interfaces. *IEEE Trans Nano Technol*, 2004, 3(2): 311
- [18] Watanabe T. Nano plating: microstructure control theory of plated film and data base of plated film microstructure. Netherlands: Elsevier, 2004: 97
- [19] Gadzuk J W, Plummer E W. Field emission energy distribution (FEED). *Reviews of Modern Physics*, 1973, 45(3): 487
- [20] Bonard J M, Salvétat J P, Stockli T, et al. Field emission from carbon nanotubes: perspectives for applications and clues to the emission mechanism. *Appl Phys A*, 1999, 69: 245
- [21] Zhang X X, Zhu C C, Zeng F G. Electron emission from printed carbon nanotube film. *Chinese Journal of Liquid Crystals and Displays*, 2008, 23(5): 612 (in Chinese)